



LAWRENCE  
LIVERMORE  
NATIONAL  
LABORATORY

# Fast Prediction of HCCI and PCCI Combustion with an Artificial Neural Network-Based Chemical Kinetic Model

W. T. Piggott, S. M. Aceves, D. L. Flowers, J. Y.  
Chen

September 28, 2007

Western States Section Meeting of the Combustion Institute  
Livermore, CA, United States  
October 16, 2007 through October 17, 2007

## **Disclaimer**

---

This document was prepared as an account of work sponsored by an agency of the United States Government. Neither the United States Government nor the University of California nor any of their employees, makes any warranty, express or implied, or assumes any legal liability or responsibility for the accuracy, completeness, or usefulness of any information, apparatus, product, or process disclosed, or represents that its use would not infringe privately owned rights. Reference herein to any specific commercial product, process, or service by trade name, trademark, manufacturer, or otherwise, does not necessarily constitute or imply its endorsement, recommendation, or favoring by the United States Government or the University of California. The views and opinions of authors expressed herein do not necessarily state or reflect those of the United States Government or the University of California, and shall not be used for advertising or product endorsement purposes.

2007 Fall Meeting of the Western States Section of the Combustion Institute  
Sandia National Laboratories, Livermore, CA  
October 16 & 17, 2007.

## Fast Prediction of HCCI and PCCI Combustion with an Artificial Neural Network-Based Chemical Kinetic Model

*W. Tom Piggott<sup>1</sup>, Salvador M. Aceves<sup>1</sup>, Daniel Flowers<sup>1</sup>, and J.Y. Chen<sup>2</sup>*

*<sup>1</sup>Department Lawrence Livermore National Laboratory  
Livermore, California 94551, USA*

*<sup>2</sup>Department of Mechanical Engineering, University of California at Berkeley,  
Berkeley, California 94720-1740, USA*

We have added the capability to look at in-cylinder fuel distributions using a previously developed ignition model within a fluid mechanics code (KIVA3V) that uses an artificial neural network (ANN) to predict ignition (The combined code: KIVA3V-ANN). KIVA3V-ANN was originally developed and validated for analysis of Homogeneous Charge Compression Ignition (HCCI) combustion, but it is also applicable to the more difficult problem of Premixed Charge Compression Ignition (PCCI) combustion. PCCI combustion refers to cases where combustion occurs as a nonmixing controlled, chemical kinetics dominated, autoignition process, where the fuel, air, and residual gas mixtures are not necessarily as homogeneous as in HCCI combustion.

This paper analyzes the effects of introducing charge non-uniformity into a KIVA3V-ANN simulation. The results are compared to experimental results, as well as simulation results using a more physically representative and computationally intensive code (KIVA3V-MPI-MZ), which links a fluid mechanics code to a multi-zone detailed chemical kinetics solver. The results indicate that KIVA3V-ANN produces reasonable approximations to the more accurate KIVA3V-MPI-MZ at a much reduced computational cost.

### 1. Introduction

Homogeneous Charge Compression Ignition (HCCI) engines are under consideration as a future technology alternative to Diesel and Spark Ignition engines due to the possibility of achieving high efficiency with substantially lower NO<sub>x</sub> and particulate emissions [1-3]. Barriers to practical implementation exist, such as high rates of heat release and high peak cylinder pressures, which limit the power output of an HCCI engine. In addition, HCCI engines tend to output high unburned hydrocarbon and carbon monoxide (CO) emissions. It is desirable to attempt to extend HCCI into a region where it could provide a higher specific power output, particularly for use with heavy truck engines. Composition stratification in particular may be used to extend the burn duration at higher loads, as well as extending the low load operating range [4, 5]. This particular strategy of allowing fuel-air mixtures with composition inhomogeneity while retaining chemical kinetics dominated ignition has been described as premixed charge compression ignition (PCCI) [6].

The nature of HCCI as chemically kinetically dominated, with little effect of turbulent mixing, makes it possible to produce effective detailed chemical kinetics based models that are less computationally expensive than SI or diesel modeling [7]. However, accurate modeling of the chemical kinetics still entails considerable computational power, to capture the chemical and fluid mechanics detail required for an accurate model. Previous work has reduced the computational cost of this modeling by using a multi-zone model with a sequential coupling of fluid mechanics to a multi-zone chemical approach [8]. However, these approaches still require considerable computational time to complete, so other methods have been tried to provide reduced but still accurate models that enable less computationally intensive simulations. One such approach is to use an artificial neural network (ANN) to model the combustion coupled with a fluid mechanics code (KIVA3V) [7]. This paper extends that work by applying fuel distributions in the cylinder to model PCCI combustion coupled with an ANN model for combustion.

## 2. Simulation Setup

The ANN setup and tuning is detailed in previous work [7]. The ANN is an approximator for non-linear functions that provides an output based on a specified set of input parameters and a training procedure. The neural network used in this study predicts ignition delay,  $\tau$ , which is the time required for a fuel-air mixture to release half of the available chemical heat at constant pressure. The input parameters used for the ANN model are temperature (T), pressure (p), equivalence ratio ( $\phi$ ), and residual gas fraction (EGR), and can be seen in Figure 1 [7].

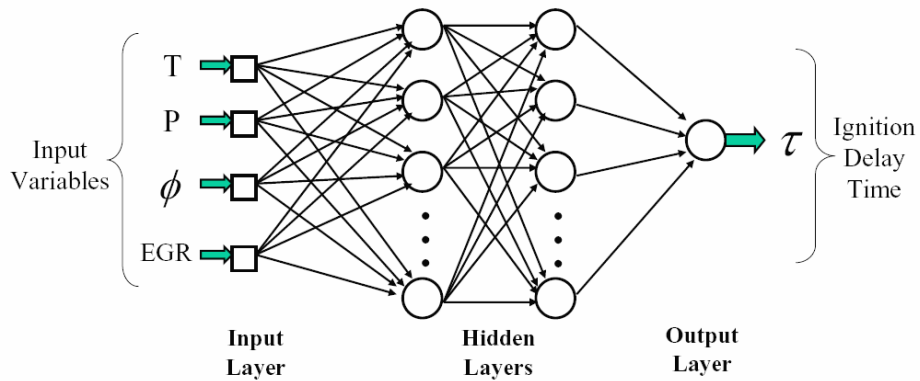


**Figure 1. Schematic depiction of the Artificial Neural Network Setup**

The ignition integral shown below in equation 1, calculates ignition based on the ignition delay time history during a given thermodynamic process (here the compression stroke) [9]. Typically, ignition is considered to occur in a mixture of fuel and air when  $I(t)$  equals 1, however for our study ignition is set when  $I(t) = 0.7$  as explained later.

$$I(t) = \int_0^t \frac{1}{\tau(T, p, \phi, EGR)} dt \quad (1)$$

The same neural network training was used as in the earlier study validated with a homogeneous fuel-air distribution [7]. Training the network requires conducting many zero-dimensional constant volume reactor simulations where important combustion parameters. A detailed iso-octane chemical kinetic mechanism was used to train the network. The operating regime used for the training was specified as follows using 38,800 points:

$$600 \text{ K} \leq T \leq 1500 \text{ K}$$

$$1 \text{ bar} \leq p \leq 200 \text{ bar}$$

$$0.1 \leq \phi \leq 0.45$$

$$0 \leq \text{EGR} \leq 0.2$$

The neural network implemented in the KIVA3V-ANN setup calculates the ignition delay for every cell in the computational mesh. It should be noted that the ignition integral information is not advected or diffused between cells. When the ignition integral of the cell reaches the specified 0.7 value mentioned earlier, combustion begins. The selection of the lower value is used since the ANN was trained using 50% heat release to predict the start of combustion. Also, the KIVA3V-ANN model used does not predict pre-ignition chemistry, which has been shown to introduce a significantly shorter ignition delay time [10]. Combustion of iso-octane is calculated using the following 2-step mechanism (note this occurs only in ignited cells) [11]:



Table 1 lists the chemical kinetic constants and reaction rates used, which were identical to those used previously [7].

**Table 1. Chemical kinetic constants and reaction rates used for Equations 2 and 3. C is the pre-exponential factor and E is the activation temperature in K.**

Reaction	C	E	Reaction Rate
Equation 2, forward	$5.7 \times 10^{11}$	$1.51 \times 10^4$	$C \exp(-E/T) [\text{C}_8\text{H}_{18}]^{0.25} [\text{O}_2]^{1.5}$
Equation 2, backward	0	0	0
Equation 3, forward	$1.0 \times 10^{10}$	$2.0 \times 10^4$	$C \exp(-E/T) [\text{CO}]^{1.0} [\text{H}_2\text{O}]^{0.5} [\text{O}_2]^{0.25}$
Equation 3, backward	$5.0 \times 10^7$	$2.0 \times 10^4$	$C \exp(-E/T) [\text{CO}_2]^{1.0}$

The geometry and operating conditions used for the study come from the Sandia HCCI engine [12]. The engine is a Cummins B-series medium-duty diesel production engine modified to operate on a single cylinder with an axisymmetric piston that provides a large squish clearance and minimum top ring-land crevice volume of 1.4% of the top dead center (TDC) volume. The

compression ratio used is 17.63:1, and the other engine specifications can be found in Table 2. The experiments kept ignition timing fixed at a few degrees before top dead center, and using an equivalence ratio between 0.04 and 0.26. The only equivalence ratios analyzed here are 0.10, 0.16, 0.20, and 0.26, as these falls within the range that the neural network is trained for.

**Table 2. Operating parameters for the Cummins B engine used in the Sandia experiments.**

Displaced volume, cm <sup>3</sup>	981
Bore, mm	102
Stroke, mm	120
Connecting rod length, mm	192
Compression ratio	17.63:1
Exhaust valve open	60° BBDC
Exhaust valve close	8° ATDC
Inlet valve open	3° BTDC
Inlet valve close	25° ABDC
Engine speed, rpm	1200
Fuel	Iso-octane
Equivalence ratio	0.04-0.26
Absolute intake pressure, bar	1.2

A schematic of the cylinder can be seen in Figure 2, with the computational mesh used shown in Figure 3.

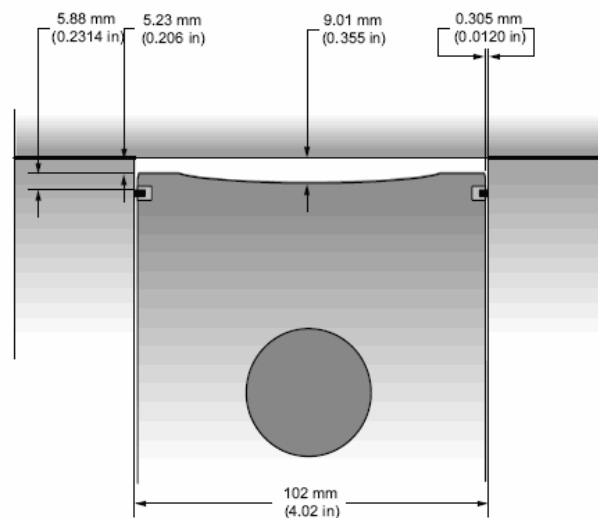


**Figure 2. Cylinder Schematic for Sandia modified Cummins B engine.**

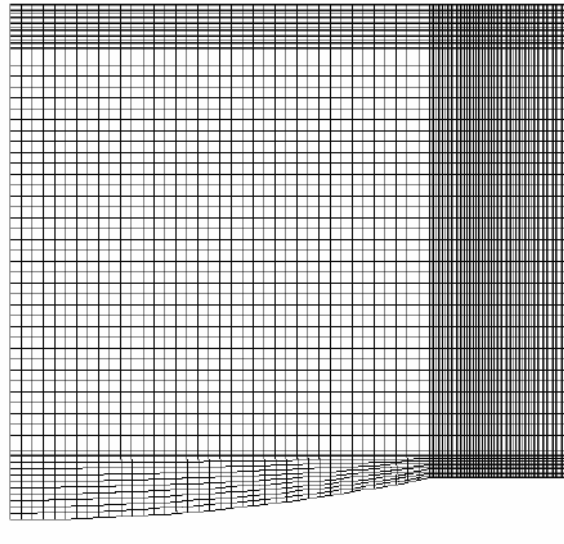


**Figure 3. View of axisymmetric KIVA3V-ANN mesh used shown at 60 degrees before TDC. At bottom dead center the grid has 51000 elements.**

Distribution of fuel and air has been implemented to enable the study of the effect of a non-homogeneous fuel distribution in the cylinder, similar to the distribution tested for the multi-zone model [6]. The stratified mixtures are achieved by imposing a distribution on the equivalence ratio that varies linearly from the cylinder centerline to the cylinder liner, as used previously [6, 13, 14]. Three distributions are imposed at the point of intake valve closure, identified as homogeneous, shallow, and steep. The homogeneous distribution is a uniform distribution that is identical to that used in earlier pure HCCI simulations. The shallow distribution has a local equivalence ratio at the centerline that is double the overall equivalence ratio, with the local equivalence ratio at the wall being one-half the average equivalence ratio. The steep distribution has a centerline equivalence ratio of three times the average equivalence ratio, with an equivalence ratio of zero at the wall. As these distributions are imposed before ignition, mixing as the compression stroke progresses affects the local distributions. Figures 4 shows the different distributions used in the KIVA3V-ANN and PCCI study.

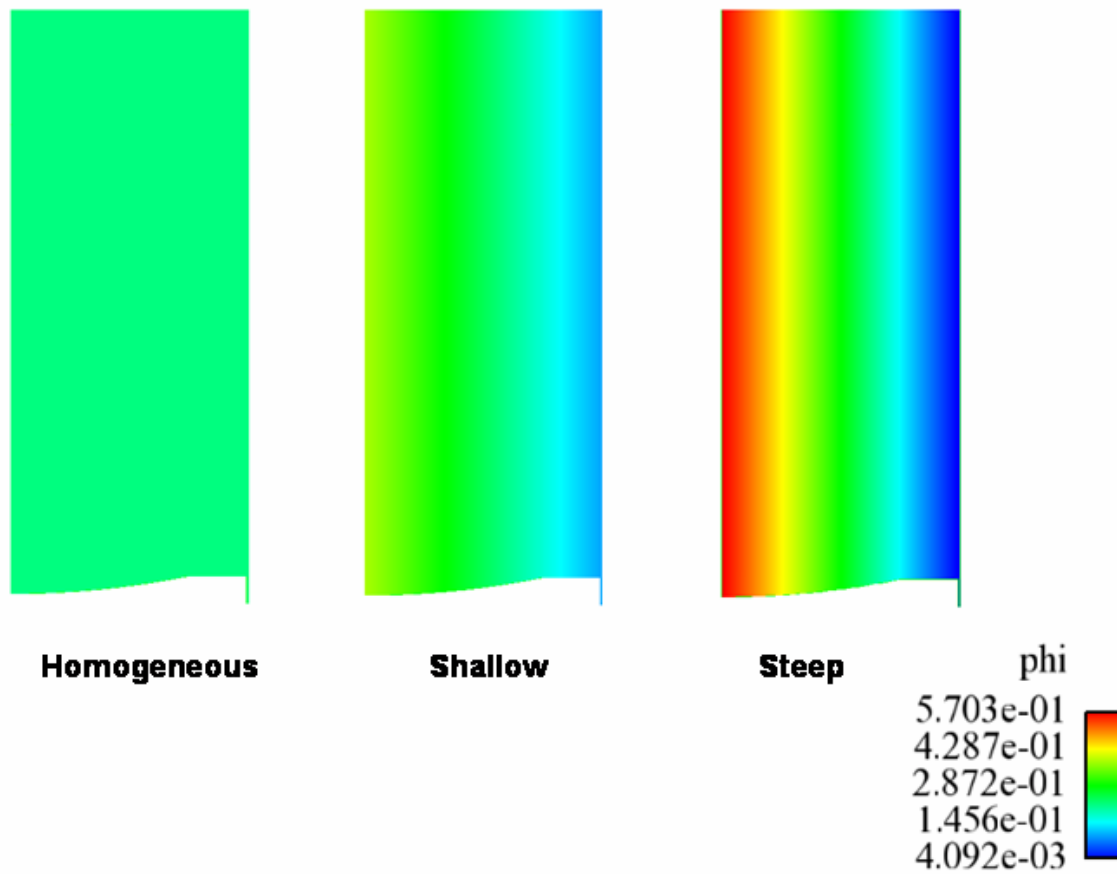


**Figure 4. Equivalence ratio distributions for three analyzed stratifications for  $\phi=0.2$**

### 3. Results

Figures 5-8 show pressure traces at varying equivalence ratios for the KIVA3V-ANN and Multi-zone simulations, as well as the experimental results from the Sandia experiment. The figures show experimental results (dotted line), neural network results (solid lines), and multi-zone results (dashed lines).



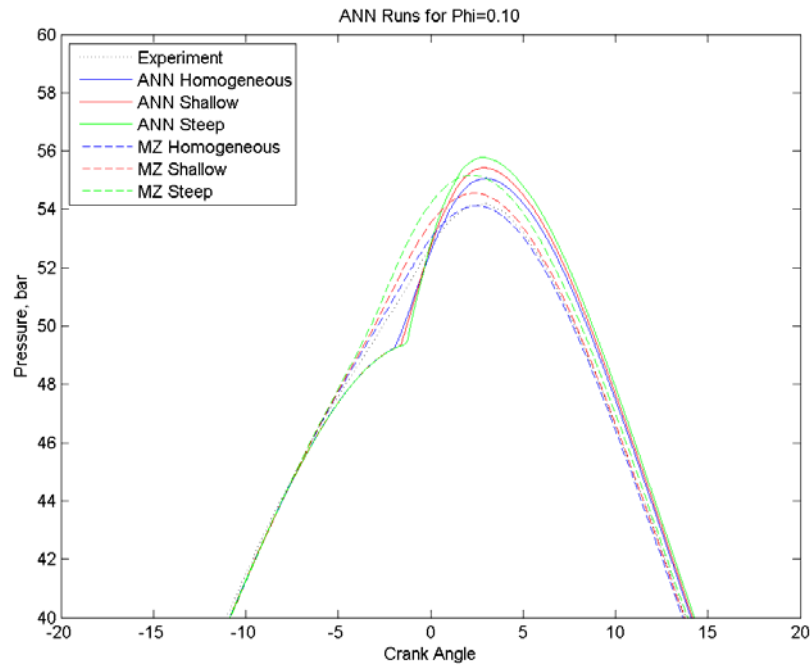


Figure 5. Pressure vs. Crank Angle for  $\phi=0.10$ . The figure shows experimental results (dotted line), neural network results (solid lines), and multi-zone results (dashed lines).

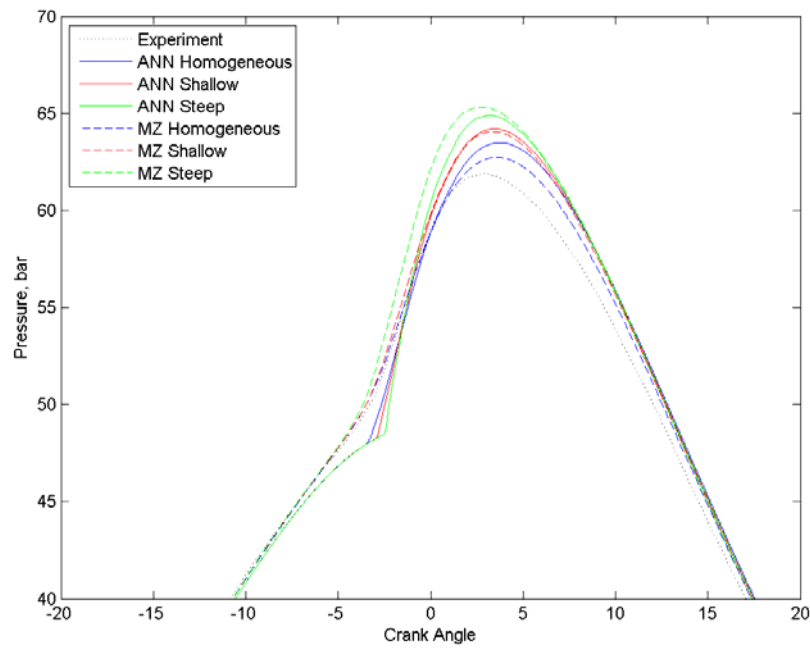


Figure 6. Pressure vs. Crank Angle for  $\phi=0.16$ . The figure shows experimental results (dotted line), neural network results (solid lines), and multi-zone results (dashed lines).

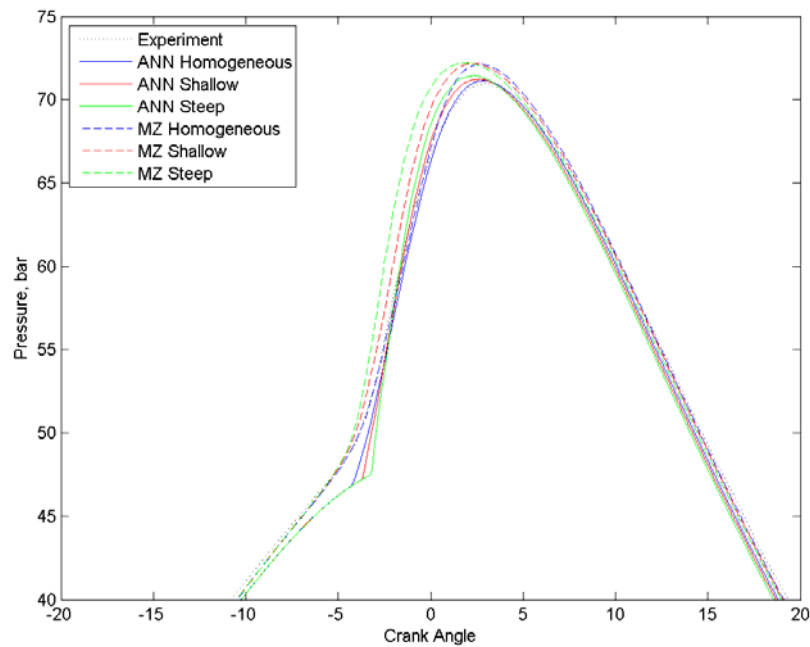


Figure 7. Pressure vs. Crank Angle for  $\phi=0.20$ . The figure shows experimental results (dotted line), neural network results (solid lines), and multi-zone results (dashed lines).

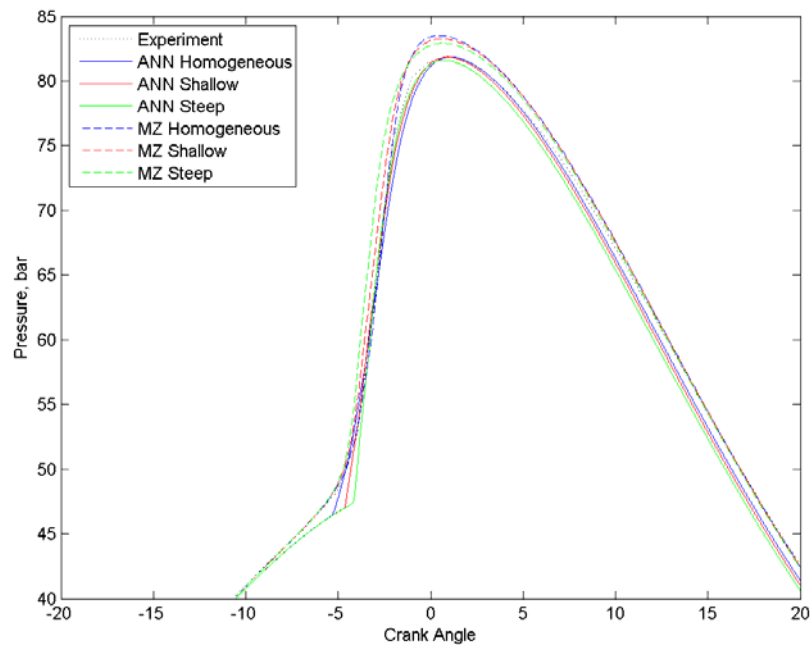


Figure 8. Pressure vs. Crank Angle for  $\phi=0.26$ . The figure shows experimental results (dotted line), neural network results (solid lines), and multi-zone results (dashed lines).

The neural network results show good agreement with the experimental results; however the multi-zone results more closely match the experiments. The neural network does not capture

low temperature heat release, and so underpredicts the experiment and multi-zone model early in the combustion process. The fast burn that occurs within the KIVA3V-ANN model is also visible in the figures 5-8, as the sudden slope change when the KIVA3V-ANN initiates combustion. For lower equivalence ratios, this fast combustion leads to an overshoot of the experimental results in the later stages of combustion. This is due to the fact that raising the equivalence ratio near the centerline results in locally increased temperatures, which leads to faster and more complete combustion. As the average equivalence ratio rises, this effect is less dominant. The stratification effect can be seen in that the homogeneous cases have the lowest peak pressure, which increases for the shallow case, and is the highest for the steep distributions.

The KIVA3V-ANN setup does not predict non-fuel hydrocarbon production because the mechanism considers only fuel once the ignition criteria is met. However, it can predict CO, CO<sub>2</sub>, and unburned fuel present in the emissions. Figures 9-11 show the percentage of fuel carbon into hydrocarbons, CO, and CO<sub>2</sub>.

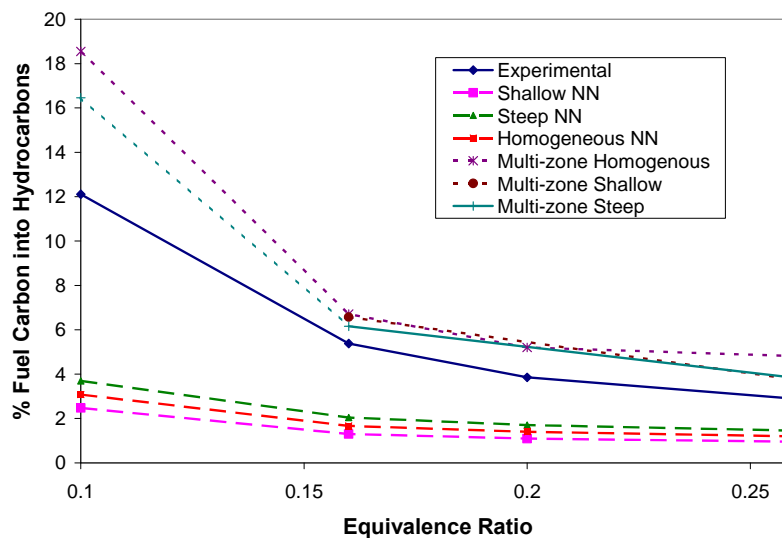


Figure 9. Percentage of Fuel Carbon into Hydrocarbons (note KIVA3V-ANN only predicts unburned fuel)

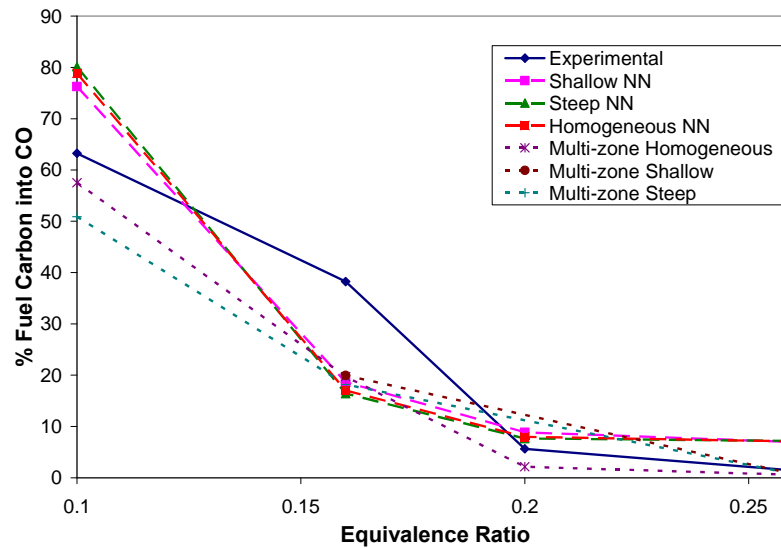


Figure 10. Percentage of Fuel Carbon into CO Emissions

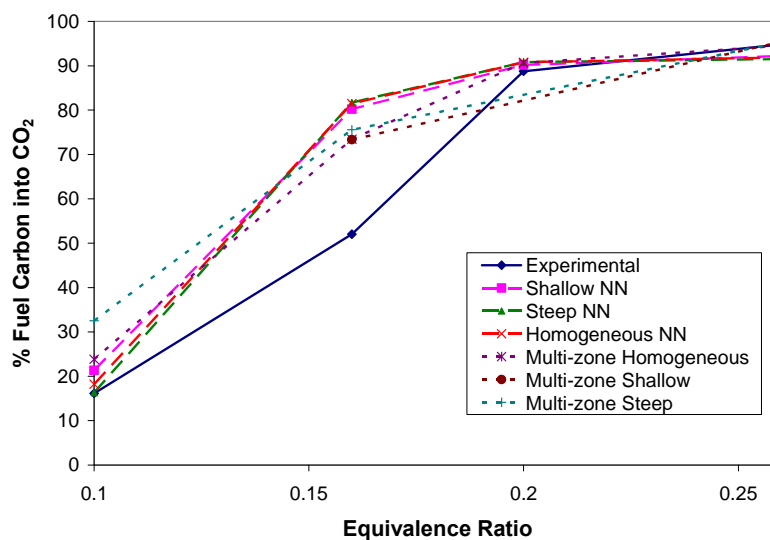


Figure 11. Percentage of Fuel into CO<sub>2</sub> Emissions

Figure 9 show a comparison of hydrocarbon emissions for KIVA3V-ANN simulation, multizone simulation, and experiment. Note that KIVA3V-ANN only considers fuel, while the experiment and multi-zone model resolve all hydrocarbons. KIVA3V-ANN tends to underpredict the amount of unburned fuel, particularly at lower equivalence ratios, but this could be expected due to the simplified mechanism for combustion used. Also, it should be noted again that the KIVA3V-ANN model does not predict oxygenated hydrocarbon production. The steep distribution shows the largest amount of unburned fuel, possibly due to the lower equivalence ratios near the cylinder edge and crevice region. The KIVA3V-ANN model shows good agreement with the experiment and multi-zone models for CO and CO<sub>2</sub> production, particularly at the higher equivalence ratios, with small differences seen among the stratified cases. Disagreement at the lowest equivalence ratio of 0.10 could be due to the neural network's training cases starting at

$\phi=0.10$ , so these cases are on the very edge of the range that the model is prepared to handle. An important note is that the KIVA3V-ANN model also does not include  $\text{NO}_x$  formation chemistry at this time.

#### 4. Conclusions

This paper showed the use of an artificial neural network combustion model applied to HCCI and PCCI combustion cases. This KIVA3V-ANN combustion model keeps track of the ignition delay time history to predict combustion. Once the combustion threshold is reached, a two-step chemical kinetic mechanism is used to predict the combustion behavior of ignited cells. The following conclusions have been seen:

1. KIVA3V-ANN has been compared with a previous experiment, and shows reasonable predictions for combustion and emissions (with emissions predictions limited to those present in the KIVA3V-ANN model). These results also compared well with previous results using a multi-zone model with more extensive chemistry, although the multi-zone results did tend to more closely track the experimental data.
2. KIVA3V-ANN as seen previously [7], predicts fast combustion and overpredicts peak cylinder pressure, with the stratified cases predicting higher peak pressures as the stratification increases (shallow to steep case).
3. The KIVA3V-ANN model underpredicts hydrocarbon emissions (and the mechanism does not include oxygenated hydrocarbon production.)
4. The KIVA3V-ANN model as implemented does not include low-temperature heat release, and so tends to underpredict pressure in the early stages of combustion. Also due to the sudden switch upon reaching the specified trigger in the ignition integral, the pressure traces show a clear change in slope as combustion begins to occur throughout the cylinder for the KIVA3V-ANN model. This may introduce larger errors when analyzing HCCI/PCCI combustion of low octane fuels (n-heptane, diesel).
5. KIVA3V-ANN gives reasonable prediction of non-homogeneous PCCI combustion with iso-octane with much lower computational effort than full chemical kinetics simulation.

#### Acknowledgments

This work was performed under the auspices of the U.S. Department of Energy by University of California, Lawrence Livermore National Laboratory under Contract W-7405-Eng-48.

#### References

- [1] P. M. Najt, D. E. Foster. SAE Paper 830264, 1983.
- [2] R. H. Thring. SAE Paper 892068, 1989.
- [3] M. Christensen, B. Johansson, and P. Einewall. SAE Paper 972874, 1997.
- [4] J. E. Dec, M. Sjöberg. SAE Paper 2003-01-0752, 2003.
- [5] J. M. Grenda. SAE Paper 2005-01-3722, 2005.
- [6] D. L. Flowers, S. M. Aceves, A. Babajimopoulos. SAE Paper 2006-01-1363, 2006.
- [7] S. M. Aceves, D. L. Flowers, J.-Y. Chen, A. Babajimopoulos. SAE Paper 2006-01-3298, 2006.
- [8] S. M. Aceves, D. L. Flowers, C. K. Westbrook, J. R. Smith, W. J. Pitz, R. Dibble, M. Christensen, B. Johansson. SAE Paper 2000-01-0327, 2000.

- [9] J. C. Livengood, P. C. Wu. *Proceedings of the Combustion Institute* 5 (1955) 347-356.
- [10] R. Ogink. *Proceedings of the 7<sup>th</sup> SAE International Conference on Engines for Automobile, ICE2005, Paper 2005-24-37*, 2005.
- [11] C. K. Westbrook, F. L. Dryer. *Combustion Science and Technology* 27(1981) 31-43.
- [12] J. E. Dec, M. Sjöberg. SAE Paper 2003-01-0752, 2003.
- [13] S. M. Aceves, D. L. Flowers, F. Espinosa-Loza, A. Babajimopoulos, D. N. Assanis. SAE Paper 2005-01-0115, 2005.
- [14] A. Babajimopoulos, D. L. Flowers, D. N. Assanis, S. M. Aceves, R. P. Hessel. *International Journal of Engine Research* vol. 6 #5 (2005) 497-512.